Chemical Physics Letters 870 (2025) 142075

Contents lists available at ScienceDirect

Chemical Physics Letters

journal homepage: www.elsevier.com/locate/cplett

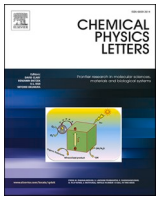

Key spectroscopic features of pyrazine lowest-lying $^1B_{1u}$ and $^1B_{2u}$ states

L.V.S. Dalagnol [a], E. Bandeira [a], N.C. Jones [b], S.V. Hoffmann [b], M.H.F. Bettega [a,*], P. Limão-Vieira [a,c,*]

[a] Departamento de Física, Universidade Federal do Paraná, Caixa Postal 19044, 81531-980 Curitiba, Paraná, Brazil
[b] ISA, Department of Physics and Astronomy, Aarhus University, Ny Munkegade 120, DK-8000, Aarhus C, Denmark
[c] Atomic and Molecular Collisions Laboratory, CEFITEC, Department of Physics, NOVA School of Science and Technology, Universidade NOVA de Lisboa, 2829-516 Caparica, Portugal

ARTICLE INFO

Keywords:
Pyrazine
Photoabsorption
Cross-sections
Theoretical calculations
Spectroscopy

ABSTRACT

We report new spectral assignments from a high-resolution vacuum ultraviolet (VUV) photoabsorption spectrum of pyrazine ($C_4H_4N_2$) lowest-lying valence excitations $\left(1^1B_{1u}\leftarrow\tilde{X}^1A_g\right)$ and $\left(1^1B_{2u}\leftarrow\tilde{X}^1A_g\right)$ in the photon energy range 3.7–6.2 eV (330–200 nm). The electronic state spectroscopy of $C_4H_4N_2$ has been investigated together with quantum chemical calculations at the time-dependant density functional theory (TD-DFT) providing vertical excitation energies and oscillator strengths. The vibronic excitation in the $^1B_{1u}$ and $^1B_{2u}$ states is accompanied by fine structure assigned to C–H stretching, $\nu'_1(a_g)$, C–C stretching, $\nu'_2(a_g)$, C–H bending, $\nu'_3(a_g)$, ring breathing, $\nu'_4(a_g)$, and ring deformation $\nu'_5(a_g)$ modes. Harmonic frequencies for pyrazine neutral electronic ground- and first excited-states have been obtained at the B3LYP/aug-cc-pVTZ level of theory. Absolute photoabsorption cross-section values are also reported from 3.7 up to 10.8 eV (310–113 nm) and compared with previous data in the literature.

1. Introduction

Pyrazine ($C_4H_4N_2$), also known as 1,4-diazine, is isoelectronic with benzene and pyrimidine (1,3-diazine), the latter with relevant implications as e.g. a benchmark molecular compound for the building blocks of DNA/RNA pyrimidines, i.e. thymine, cytosine and uracil. In 2010 we reported a comprehensive description of the electronic state spectroscopy of pyrimidine by photoabsorption and electron energy loss spectroscopies, together with electron scattering experiments [1]. This previous work motivated us to investigate other nitrogen heterocyclic aromatic compounds, such as pyrazine.

Detailed information and description of the electronic states of a molecule are essential to understand the underlying mechanisms governing the intricate intramolecular dynamics triggered by electron and photon interactions, see e.g. [2,3] and references therein. The pyrazine molecule has been widely investigated by gas-phase VUV absorption in the energy range from 3.5 up to 12.0 eV [4–13], infrared and Raman spectroscopies [4,5,10], phosphorescence and photoexcitation [14] and the effects of molecular rotation on the $S_1 \longleftarrow S_0$ excitation [5,15–17]. Also, we note relevant theoretical studies on the vertical excitation energies [18–22] and photo induced dynamics of the lowest singlet states [2,20,22,23]. Finally, information on vibrational modes from photoelectron spectroscopy have been reported [24–28]. Notwithstanding, there are either inconsistencies in the assignments, or new spectral features observed here for the first time for the two lowest-energy absorption bands, that need to be comprehensively discussed.

In this Letter we combine experimental and theoretical methods on the assignment of the lowest-lying excited electronic states of pyrazine, $^1B_{1u}$ and $^1B_{2u}$, by high-resolution VUV radiation provided from a synchrotron light source in the photon energy range 3.7–6.2 eV. Absolute photoabsorption cross-sections have been obtained in a wider range, 3.7–10.8 eV, while time-dependant density functional theory (TD-DFT/B3LYP/aug-cc-pVTZ) calculations provide energies and oscillator strengths for the lowest-lying neutral states.

2. Experimental method

The AU-UV beam line of the ASTRID2 synchrotron facility at Aarhus University, Denmark was used to obtain a high-resolution VUV photoabsorption spectrum of pyrazine in the energy range from 3.7 eV up to

* Corresponding authors at: Departamento de Física, Universidade Federal do Paraná, Caixa Postal 19044, 81531-980 Curitiba, Paraná, Brazil.
E-mail addresses: bettega@fisica.ufpr.br (M.H.F. Bettega), plimaovieira@fct.unl.pt (P. Limão-Vieira).

https://doi.org/10.1016/j.cplett.2025.142075
Received 11 February 2025; Received in revised form 27 March 2025; Accepted 28 March 2025
Available online 4 April 2025

10.8 eV (Fig. 1). The absorption gas cell end station used to perform the experiments has been described before [29,30]. Briefly, synchrotron radiation passes through a static gas sample filled with pyrazine vapour at room temperature with the transmitted light detected by a photomultiplier tube (PMT). At both ends of the absorption cell, MgF_2 transmission windows set the low wavelength detection limit to 115 nm. The gas sample number density in the absorption cell is obtained by recording the absolute pressure of pyrazine measured by a capacitance manometer (Chell CDG100D), while the absorption cross-sections were measured in the pressure range 0.02–1.27 mbar, to achieve attenuations of 50 % or less and hence avoiding saturation effects.

The absolute photoabsorption cross-sections values, σ, in units of megabarn (1 Mb $\equiv 10^{-18}$ cm^2) were obtained from the Beer-Lambert attenuation law, $I_t = I_0 e^{(-N\sigma l)}$, where I_t is the light intensity transmitted through the gas sample, I_0 is that through the evacuated cell, N the molecular number density of $C_4H_4N_2$, and l the absorption path length (15.5 cm). Throughout the collection of each spectrum, the synchrotron beam current was monitored, and background scans, I_0, were recorded with the cell evacuated. ASTRID2 operates in a "top-up" mode allowing the light intensity to be kept quasi-constant, thus compensating for the constant beam decay in the storage ring. The variations (2–3 %) of the incident flux are therefore normalized to the beam current in the storage ring. Following the methodology employed, within the wavelength region scanned (115–310 nm), accurate cross-section values are obtained by recording the VUV spectrum in small (5 or 10 nm) sections, allowing an overlap of at least 10 data points between the adjoining sections and optimising the pressure used according to the cross-section of the features. This methodology allows us to determine photoabsorption cross-sections to an accuracy of ±5 %. For a detailed description related to the uncertainties see ref. [31]. The resolution in the present spectrum is better than 0.08 nm [29], which corresponds to 1, 3, and 7 meV at the low extreme, the midpoint, and the high extreme of the photon energy range scanned, respectively.

The solid sample used in the VUV photoabsorption measurements was purchased from Sigma-Aldrich, with a stated purity of ≥99 %. The sample was used as delivered.

3. Theoretical methods

The vertical excitation energies and corresponding oscillator strengths of the most relevant electronically excited states of pyrazine were calculated employing TD-DFT [32,33] with a B3LYP functional [34–40] and the aug-cc-pVTZ basis set [41] as implemented in GAMESS-US computational package [42]. The major electronically excited states of pyrazine are in Table 1, whereas a complete list is in the Supplementary Material Table S1. We also carried out additional tests with the PBE0 [43] and CAM-B3LYP functionals [44] and the aug-cc-pVTZ [41] basis set. These results are listed in the Supplementary Material Tables S2 and S3, respectively. The choice model with B3LYP functional and the aug-cc-pVTZ basis set has been used because the results are more consistent with the experimental data.

The nature of each excitation was assessed by visual inspection of the molecular orbitals for each transition. Additionally, harmonic frequencies (B3LYP/aug-cc-pVTZ) for the neutral electronic ground-state (Table S2) and the neutral electronic first excited-state (Table S3) have also been obtained, where a scaling factor for B3LYP/aug-cc-pVDZ of 0.967 provided by Kashinski et al. [45] has been applied.

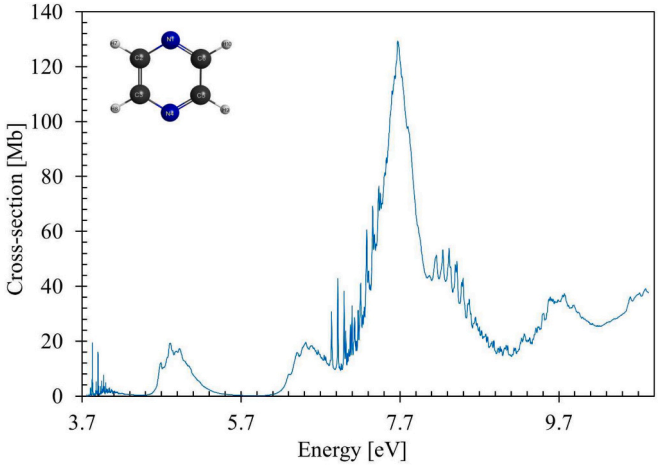

Fig. 1. The high-resolution photoabsorption spectrum of pyrazine in the 3.6–10.8 eV photon energy range. The pyrazine molecular structure was obtained with MacMolPlt graphical interface [47]. See text for details.

4. Structure and properties of pyrazine

The neutral ground-state and neutral first excited-state geometries of pyrazine obtained at the B3LYP/aug-cc-pVTZ level, together with their bond lengths (Å) and bond angles (°) are listed in the Supplementary Material (Figs. S1 and S2). The calculated outermost electronic configuration of the $\widetilde{X}^1A_g$ ground-state (Fig. S1) is … $(5a_g)^2$ $(3b_{2u})^2$ $(4b_{3u})^2$ $(4b_{2u})^2$ $(1b_{1u})^2$ $(3b_{1g})^2$ $(1b_{2g})^2$ $(5b_{3u})^2$ $(1b_{3g})^2$ $(6a_g)^2$. The ground-state MO character displayed in Fig. S3 show the highest occupied molecular orbital (HOMO), $6a_g$, is the N $2p$ lone pair orbital $(\overline{n}_N)$ in the molecular plane. The second highest occupied molecular orbital (HOMO–1), $1b_{3g}$, and (HOMO–3), $1b_{2g}$, are $(\pi_{CN/CC})$, (HOMO–4), $3b_{1g}$, is (π_{CC}/σ_{CN}) whereas (HOMO–2), $5b_{3u}$, is $(\overline{n}_N)$ in character. Other MOs from which electrons can be excited (HOMO-5), $1b_{1u}$, is (π_{ring}), (HOMO–6), $4b_{2u}$, (HOMO–7), $4b_{3u}$, and (HOMO–9), $5a_g$, are mainly $(\sigma_{CN/CC}/\sigma_{CH})$. Finally, (HOMO–8), $3b_{2u}$, is mostly (π_{CN}) bonding in character. The main absorption features in Fig. 1 are due to electronic excitations from these MOs to valence, mixed valence-Rydberg and Rydberg orbitals, with the calculated dominant excitation energies and oscillator strengths listed in Table S1.

We have also obtained additional information from the calculation of the harmonic frequencies and labelling for the neutral and the lowest-lying electronic excited states and compared with the available data in the literature (see Tables S2 and S3). The fine structure of the main modes in $\left(1^1B_{1u}\leftarrow\widetilde{X}^1A_g\right)$ and $\left(1^1B_{2u}\leftarrow\widetilde{X}^1A_g\right)$ absorption bands have been assigned based on the energies (and wavenumbers) in the neutral electronic ground-state to 0.379 eV (3055 cm^{-1}) for the C–H stretching, $\nu''_1(a_g)$, 0.196 eV (1580 cm^{-1}) for C–C stretching, $\nu''_2(a_g)$, 0.153 eV (1233 cm^{-1}) for C–H bending, $\nu''_3(a_g)$, 0.126 eV (1016 cm^{-1}) for ring breathing, $\nu''_4(a_g)$ and 0.075 eV (602 cm^{-1}) for ring deformation $\nu''_5(a_g)$ [5]; with the corresponding modes in the electronic first excited-state to 0.388 eV (3126 cm^{-1}) for $\nu'_1(a)$, 0.148 eV (1190 cm^{-1}) for $\nu'_9(a)$, 0.146 eV (1177 cm^{-1}) for $\nu'_{10}(a)$, 0.174 eV (1406 cm^{-1}) for $\nu'_5(a)$ and 0.090 eV (728 cm^{-1}) for $\nu'_{16}(a)$, respectively (see Table S3).

Following our implemented methodology when dealing with the assignment of fine structure, the X^n_m notation, with m and n denoting the initial and final vibrational states for the vibronic structure (X), is adopted. Note that more than one mode can contribute to the absorption features, thus suggesting the possibility of Fermi resonances. The MOs numbering from which electronic excitations may occur differs from Holland et al. [26] electronic configuration, however with the same character as in the present calculations.

5. Results and discussion

The complete photoabsorption spectrum of pyrazine in the energy range from 3.7 to 10.8 eV is shown in Fig. 1. A thorough spectral assignment above 6 eV can be found in references [7–9, 11, 14, 18, 46] and shall not be discussed here. Here, we only deal with the two lowest-lying excited states for which there are still either inconsistencies in the

Table 1
The main calculated vertical excitation energies (TD-DFT/B3LYP/aug-cc-pVTZ) and oscillator strengths of pyrazine compared with experimental data. Energies in eV. See text for details.

Pyrazine				E (eV) Expt.[a]	Cross-section (Mb)	E (eV) [9]
State	E (eV)	f_L	Dominant excitations			
$\widetilde{X}\ ^1A_g$						
$1\ ^1B_{1u}$	3.915	0.0048	$\pi^*_{CN/CC}(2b_{1u}) \leftarrow \overline{n}_N(6a_g)$ (100 %)	3.829	19.50	
$1\ ^1B_{2u}$	5.409	0.1036	$\pi^*_{CN/CC}(2b_{1u}) \leftarrow \pi_{CN/CC}(1b_{3g})$ (88 %), $\pi^*_{CN/CC}(1a_u) \leftarrow \pi_{CN/CC}(1b_{2g})$ (11 %)	4.806	19.35	4.806
$1\ ^1B_{3u}$	6.468	0.0557	$\pi^*_{CN/CC}(1a_u) \leftarrow \pi_{CN/CC}(1b_{3g})$ (75 %), $\pi^*_{CN/CC}(2b_{1u}) \leftarrow \pi_{CN/CC}(1b_{2g})$ (21 %)	6.51(7)	19.62	6.516
$3\ ^1B_{3u}$	7.615	0.1474	$\pi^*_{CN/CC}(2b_{1u}) \leftarrow \pi_{CN/CC}(1b_{2g})$ (49 %), $3s(7a_g) \leftarrow \overline{n}_N(5b_{3u})$ (36 %), $\pi^*_{CN/CC}(1a_u) \leftarrow \pi_{CN/CC}(1b_{3g})$ (10 %)	6.919	42.88	6.918
$4\ ^1B_{3u}$	7.796	0.2911	$3s(7a_g) \leftarrow \overline{n}_N(5b_{3u})$ (60 %), $\pi^*_{CN/CC}(2b_{1u}) \leftarrow \pi_{CN/CC}(1b_{2g})$ (22 %)	7.675	129.19	
$5\ ^1B_{2u}$	8.488	0.0548	$3p'(6b_{2u}) \leftarrow \overline{n}_N(6a_g)$ (82 %), $3p''(7b_{2u}) \leftarrow \overline{n}_N(6a_g)$ (12 %)	8.318	53.85	8.324
$9\ ^1B_{3u}$	9.518	0.0871	$3d(9a_g) \leftarrow \overline{n}_N(5b_{3u})$ (65 %), $3p(3b_{1u}) \leftarrow \pi_{CN/CC}(1b_{2g})$ (30 %)	9.770	37.26	9.764
$10\ ^1B_{1u}$	10.325	0.1398	$4p'(8b_{2u}) \leftarrow \pi_{CN/CC}(1b_{3g})$ (93 %)		39.13	

[a] the last decimal of the energy value is given in brackets for these less-resolved features;

literature or lack of any detailed vibronic assignments. The expanded views of the measured cross-sections in the 3.7–4.6 eV and in the 4.4–6.3 eV photon energy (Figs. 2 and 3) show fine structure which has been assigned to vibronic transitions, with main vibrational modes assigned according to Hewett et al. [5]. Although the low-lying excited states vibrational modes may correspond to a different symmetry point group than the ground-state, from now on we adopt the normal mode description related to the latter.

The assignments of the different absorption features listed in Tables 2 and 3 contain the electronic and the major vibrational excitations from the ground-state to the $\left(1^1B_{1u} \leftarrow \widetilde{X}^1A_g\right)$ and $\left(1^1B_{2u} \leftarrow \widetilde{X}^1A_g\right)$ electronic excited states. The TD-DFT calculated vertical excitation energies are shown in Table 1 and are compared with the experimental data. A reasonably good level of agreement to within ±9 % is noted, however for the $\left(1^1B_{2u} \leftarrow \widetilde{X}^1A_g\right)$ transition this value increases to a difference of ~12 %. Of relevance is the D_{2h} symmetry dipole forbidden absorption band between 5.6 and 6.1 eV which is not evident in the current study, but has been reported in a quantum dynamics study as a dark $A_u(\pi\pi^*)$ state [23].

5.1. The 3.7–4.6 eV photon energy range

The lowest-lying valence excitation is assigned to the promotion of the nitrogen lone pair in-plane ($\overline{n}_N$) to the $\pi^*_{CN/CC}$ antibonding orbitals, $\pi^*_{CN/CC}(2b_{1u}) \leftarrow \overline{n}_N(6a_g)$, $\left(1^1B_{1u} \leftarrow \widetilde{X}^1A_g\right)$. Fig. 2 shows the 0^0_0 origin of the band at 3.829 eV, with a cross-section of 19.50 Mb, in good agreement

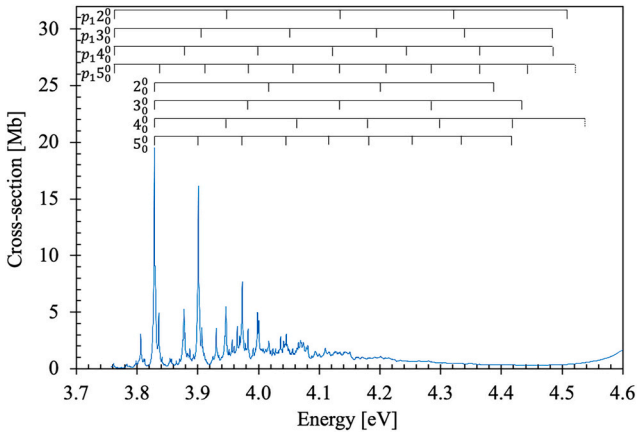

Fig. 2. Detail of the photoabsorption spectrum of pyrazine in the 3.7–4.6 eV photon energy showing progressions $p_1X^0_0$(X = 2,3,4,5) and the main active vibrational modes. See text for details.

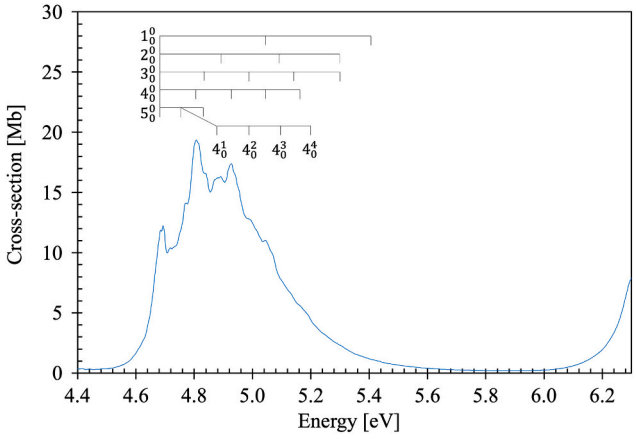

Fig. 3. Detail of the photoabsorption spectrum of pyrazine in the 4.4–6.3 eV photon energy. See text for details.

with the calculated value of 3.915 eV and an oscillator strength f_L = 0.0048 (Table 1). This has been reported from experimental data at 3.83 eV (f_L = 0.01) by Bolovinos et al. [8], at 3.759 eV from two-photon excitation [14], at 3.828 eV (30,876 cm^{-1}) from fluorescence spectroscopy [12,16], whereas quantum chemical calculations reported values from 3.78 to 4.87 eV depending on the level of theory [18,20,22,23]. The lowest calculated value of 3.16 eV and an oscillator strength (unnormalized) of 0.31 has been reported by Stener et al. [9].

He et al. [19] used multireference CAS-SCF methods to describe pyrazine's 1^1B_{1u} state by including three totally symmetric modes, C–H bending, $\nu'_3(a_g)$, ring breathing, $\nu'_4(a_g)$ and ring deformation $\nu'_5(a_g)$, together with out-of-plane C–H bending, $\nu'_8(b_{1g})$. We suggest the fine structure is due to vibronic excitation assigned to C–C stretching, $\nu'_2(a_g)$, C–H bending, $\nu'_3(a_g)$, ring breathing, $\nu'_4(a_g)$ and ring deformation $\nu'_5(a_g)$ modes, with mean energies values ($\overline{\Delta E}$) of 0.186, 0.148, 0.120 and 0.074 eV, respectively, (Table 2). Some of the vibrational assignments listed in Table 2 have not been added in Fig. 2 to avoid congestion. The band also shows progressions $p_iX^n_m$ (i = 1–3) that are listed in Table 2 and have been assigned to the contribution of C–C stretching, $\nu'_2(a_g)$, C–H bending, $\nu'_3(a_g)$, ring breathing, $\nu'_4(a_g)$ and ring deformation $\nu'_5(a_g)$ (modes)

The VUV photoabsorption energy resolution of the current experiments is not sufficient to resolve the internal rotational contributions within the $S_1 \leftarrow S_0$ transition. However, fluorescence spectroscopy experiments report a comprehensive analysis of the internal routes for energy redistribution among the available degrees of freedom, i.e., vibrational and rotational motions. In such intricate underlying

Table 2
Proposed vibrational assignments of pyrazine lowest-lying absorption band in the photon energy range 3.7–4.6 eV[a]. Energies in eV. See text for details.

Assignment	Energy	ΔE (ν'_5)	ΔE (ν'_4)	ΔE (ν'_3)	ΔE (ν'_2)
$\pi^*_{CN/CC}(2b_{1u}) \longleftarrow \overline{n}_N(6a_g)$, $\left(1^1B_{1u} \leftarrow \widetilde{X}^1A_g\right)$					
$p_1 0_0^0$	3.762	–	–	–	–
$p_2 0_0^0$	3.784	–	–	–	–
$p_3 0_0^0$	3.806	–	–	–	–
0_0^0	3.829	–	–	–	–
$p_1 5_0^1$	3.836	0.074	–	–	–
$p_2 5_0^1$	3.857	0.073	–	–	–
$p_1 4_0^1/p_3 5_0^1$	3.877	0.071	0.115	–	–
$5_0^1/p_2 4_0^1$	3.901	0.072	0.117	–	–
$p_1 3_0^1$	3.907	–	–	0.145	–
$p_1 5_0^2$	3.91(2)(s, w)	0.076	–	–	–
$p_2 5_0^2/p_3 4_0^1$	3.92(8) (s)	0.071	0.122	–	–
$p_2 3_0^1$	3.930	–	–	0.146	–
$p_1 2_0^1/p_3 5_0^2/4_0^1$	3.946	0.069	0.117	–	0.184
$p_3 3_0^1$	3.951	–	–	0.145	–
$p_2 2_0^1$	3.967	–	–	–	0.183
5_0^2	3.973	0.072	–	–	–
$3_0^1/p_1 5_0^3$	3.983	0.071	–	0.154	–
$p_3 2_0^1$	3.991	–	–	–	0.185
$p_2 5_0^3$	3.99(6) (s)	0.068	–	–	–
$p_1 4_0^2$	3.999	–	0.122	–	–
$2_0^1/p_2 4_0^2/p_3 5_0^3$	4.017	0.071	0.116	–	0.188
$p_3 4_0^2/5_0^3$	4.046	0.073	0.118	–	–
$p_1 3_0^2$	4.05(0) (s)	–	–	0.143	–
$p_1 5_0^4$	4.056	0.073	–	–	–
4_0^2	4.061	–	0.115	–	–
$p_2 5_0^4$	4.069	0.073	–	–	–
$p_2 3_0^2$	4.079	–	–	0.149	–
$p_3 5_0^4$	4.08(9) (w)	0.072	–	–	–
$p_3 3_0^2$	4.094	–	–	0.143	–
5_0^4	4.116	0.070	–	–	–
$p_2 4_0^3 5_0^5$	4.134	0.065	0.117	–	–
$p_2 2_0^2$	4.151	–	–	–	0.184
$p_3 4_0^3/p_3 5_0^5$	4.16(6) (b)	0.077	0.120	–	–
4_0^3	4.181	–	0.120	–	–
$p_1 3_0^3$	4.19(3) (s)	–	–	0.142	–
$p_1 4_0^3$	4.124	–	0.125	–	–
$p_1 5_0^5$	4.12(9) (b)	0.073	–	–	–
$p_1 2_0^2/3_0^2$	4.134	–	–	0.151	0.188
$p_3 2_0^2$	4.176	–	–	–	0.185
5_0^5	4.184	0.068	–	–	
2_0^2	4.201	–	–	–	0.184
$p_1 5_0^6/p_2 4_0^3 5_0^6/p_2 5_0^6$	4.209	0.080/ 0.075	–	–	–
$p_1 4_0^4/p_3 3_0^3$	4.24(4) (s)	–	0.120	0.150	–
$p_2 3_0^3$	4.23(2) (s)	–	–	0.153	–
$p_3 5_0^6$	4.234	0.068	–	–	–
$p_2 4_0^4$	4.25(4) (b)	–	0.120	–	–
5_0^6	4.261	0.077	–	–	–
$3_0^3/p_1 5_0^7/p_2 5_0^7/p_3 4_0^4$	4.28(6) (s)	0.077/ 0.077	0.120	0.152	–
4_0^4	4.29(8) (s)	–	0.117	–	–
$p_3 5_0^7$	4.30(7) (w)	0.073	–	–	–
$p_1 2_0^3$	4.320	–	–	–	0.186
$p_2 2_0^3/5_0^7$	4.33(4) (b)	0.073	–	–	0.183
$p_1 3_0^4$	4.33(7) (s)	–	–	0.145	–
$p_2 4_0^5$	4.37(4) (b,w)	–	0.120	–	–
$2_0^3/p_2 3_0^4$	4.38(8) (b)	–	–	0.156	0.187
$p_1 4_0^5/p_1 5_0^8/p_2 5_0^8/p_3 2_0^3$	4.36(4) (b)	0.078/ 0.078	0.120	–	0.188
$p_3 2_0^4$	4.39(2) (b)	–	–	0.148	–
$p_3 4_0^5$	4.40(6) (b,w)	–	0.120	–	–
5_0^8	4.415	0.081	–	–	–
4_0^5	4.419	–	0.121	–	–
$3_0^4/p_1 5_0^9$	4.43(4) (w)	0.070	–	0.148	–
$p_2 5_0^9$	4.44(2) (b,w)	0.078	–	–	–
$p_1 3_0^5/p_1 4_0^6$	4.48(2) (s)	–	0.118	0.145	–
$p_2 4_0^6$	4.49(6) (w)	–	0.122	–	–
$p_1 2_0^4$	4.50(9) (s)	–	–	–	0.188
$p_1 5_0^{10}/p_2 2_0^4/p_2 5_0^9$	4.51(6) (s)	0.082/ 0.074	–	–	0.182
$p_3 4_0^6$	4.52(7) (s)	–	0.121	–	–
$4_0^6/p_2 3_0^5/p_3 2_0^5$	4.53(8) (s)	–	0.119	0.150/ 0.146	–
$p_3 2_0^4$	4.54(7)(s, w)	–	–	–	0.183
		$\overline{\Delta E}$ 0.074	0.120	0.148	0.186

[a] (s) shoulder structure; (w) weak feature; (b) broad feature (the last decimal of the energy value is given in brackets for these less-resolved features).

molecular mechanisms, internal conversions to triplet states through radiationless transitions are noted as dominant relaxation processes. For further details see Refs. [5, 15, 16].

The geometries of pyrazine in the ground-state and first excited-state, together with their bond lengths in Å and bond angles in (°), are shown in Fig. S1 and S2. Upon electronic excitation we note an increase of ~2 % in the C2–C3 and ~ 5 % in the C5–C6 bond lengths which lend support to C–C stretching $\nu'_2(a_g)$ and C–H bending $\nu'_3(a_g)$ modes assigned in Fig. 2. A modest reduction in the C2–H7 and C5–H9 interatomic distances (< 1 %) and in the Nl–C2–C3 angle (< 5 %) between the neutral ground-state and the first excited-state, are related to the ring deformation $\nu'_5(a_g)$ mode. Finally, the changes in the N1–C2–H7/ N4–C5–H9 angles from 117.23° in the ground-state to 121.84° in the first excited-state are in agreement with the ring breathing, $\nu'_4(a_g)$ mode assigned in Fig. 2.

5.2. The 4.4–6.3 eV photon energy range

The second absorption band is here better resolved than in previous VUV experiments [7–10,12,13]. It is centred at 4.806 eV with a maximum cross-section of 19.35 Mb and is assigned to the valence excitation $\pi^*_{CN/CC}(2b_{1u}) \leftarrow \pi_{CN/CC}(1b_{3g}) + \pi^*_{CN/CC}(1a_u) \leftarrow \pi_{CN/CC}(1b_{2g})$, $\left(1^1B_{2u} \leftarrow \widetilde{X}^1A_g\right)$ with an oscillator strength $f_L = 0.1036$ (Table 1). The VUV spectrum of Walker and Palmer [11] reports a value of 4.769 eV. The equation-of-motion coupled-cluster calculations report a value at 5.09 eV ($f_L = 0.08$) while Lin et al. [20] and Sala et al. [23] ab initio calculations report values from 4.64 up to 5.46 eV and 4.64 up to 5.71 eV, depending on the level of theory used.

Table 3
Proposed vibrational assignments of pyrazine valence excitation in the photon energy range 4.4–6.3 eV[a]. Energies in eV. See text for details.

Assignment	Energy	ΔE (ν'_5)	ΔE (ν'_4)	ΔE (ν'_3)	ΔE (ν'_2)	ΔE (ν'_1)
$\pi^*_{CN/CC}(1a_u) \longleftarrow \pi_{CN/CC}(1b_{2g}) + \pi^*_{CN/CC}(2b_{1u}) \longleftarrow \pi_{CN/CC}(1b_{3g}), \left(1^1B_{2u} \leftarrow \widetilde{X}^1A_g\right)$						
0^0_0	4.684	–	–	–	–	–
?	4.693	–	–	–	–	–
?	4.718	–	–	–	–	–
5^1_0	4.75(6)(s, w)	0.072	–	–	–	–
4^1_0	4.809	–	0.125	–	–	–
5^2_0	4.82(8)(s)	0.072	–	–	–	–
3^1_0	4.84(1)(s)	–	–	0.157	–	–
$5^1_0 4^1_0$	4.88(1)(b, w)	–	0.125	–	–	–
2^1_0	4.88(7)(b)	–	–	–	0.203	–
$5^2_0 4^1_0$	4.96(0)(s, w)	0.079	–	–	–	–
4^2_0	4.928	–	0.119	–	–	–
$3^2_0/5^1_0 4^2_0$	4.99(3)(s)	–	0.112	0.152	–	–
$1^1_0/4^3_0$	5.046	–	0.118	–	–	0.362
$2^2_0/5^1_0 4^3_0$	5.09(2)(s, b)	–	0.099	–	0.205	–
3^3_0	5.14(0)(s, b)	–	–	0.147	–	–
4^4_0	5.16(8)(s, w)	–	0.122	–	–	–
$5^1_0 4^4_0$	5.19(4)(s, b)	–	0.102	–	–	–
$2^3_0/3^4_0$	5.30(3)(s, w)	–	–	0.163	0.211	–
1^2_0	5.40(9)(b, w)	–	–	–	–	0.363
	$\overline{\Delta E}$	0.074	0.115	0.155	0.206	0.363

[a] (s) shoulder structure; (w) weak feature; (b) broad structure (the last decimal of the energy value is given in brackets for these less-resolved features); (?) means unassigned feature.

The 0^0_0 origin band is assigned at 4.684 eV (Table 3 and Fig. 3), the absorption data of Innes et al. [46] and Yamazaki et al. [12] report it at 4.692 eV, Suzuka and co-workers [10] at 4.700 eV, while there is an excellent agreement with the value of 4.685 eV from Stener and co-workers [9]. The band is mainly accompanied by excitation of C–H stretching, $\nu'_1(a_g)$, C–C stretching, $\nu'_2(a_g)$, C–H bending, $\nu'_3(a_g)$, ring breathing, $\nu'_4(a_g)$ and ring deformation $\nu'_5(a_g)$ modes, with mean energy values of 0.363, 0.206, 0.155, 0.115 and 0.074 eV (Table 3). We also assigned a combination band involving $\nu'_4(a_g)$ and $\nu'_5(a_g)$ modes, however there are a few features that have not been assigned in Table 3 (noted as "?") but can be part of the progressions.

5.3. Absolute photoabsorption cross sections

The present absolute ultraviolet photoabsorption cross-sections of pyrazine are reported in the photon energy region 4.0–10.8 eV, with Table 1 listing the major electronic transitions and their values in units of Mb. Samir et al. [13] reported cross-section values at 3.911 eV (317 nm) and 4.843 eV (256 nm) of 2.2 and 12.4 Mb, relative to the present respective values of 1.25 and 16.34 Mb. Bolovinos et al. [8] reported cross sections of 8.0 Mb (4.69 eV) and 10.8 Mb (6.30 eV) different from the present values of 12.10 Mb and 7.9 Mb. Stener et al. [9] vacuum ultraviolet photoabsorption cross sections are found to be in reasonable agreement with the present cross-sections in shape and magnitude, whereas Walker and Palmer [11] are consistently 25–35 % lower.

6. Conclusions

The present joint experimental and theoretical investigation of pyrazine electronic state spectroscopy provides the most complete study in the 3.7–6.2 e*V* (330–200 nm) energy range comprising the lowest-lying valence excitations $\left(1^1B_{1u} \leftarrow \widetilde{X}^1A_g\right)$ and $\left(1^1B_{2u} \leftarrow \widetilde{X}^1A_g\right)$. The features in the high-resolution absolute photoabsorption spectrum have been assigned with the help of quantum chemical calculations, on the vertical excitation energies and oscillator strengths at TD-DFT level of theory. The comprehensive analysis of the absorption structures has also allowed us to propose assignments for the C–H stretching, $\nu'_1(a_g)$, C–C stretching, $\nu'_2(a_g)$, C–H bending, $\nu'_3(a_g)$, ring breathing, $\nu'_4(a_g)$, and ring deformation $\nu'_5(a_g)$ modes. Harmonic frequencies from B3LYP/aug-cc-p*V*TZ calculations for the neutral electronic ground- and first excited-state have also been obtained. Finally, absolute cross-section values are reported from 3.7 up to 10.8 eV (310–113 nm) and compared with the available data in the literature.

CRediT authorship contribution statement

L.V.S. Dalagnol: Software, Investigation. **E. Bandeira:** Software, Investigation. **N.C. Jones:** Writing – review & editing, Supervision, Investigation, Data curation, Conceptualization. **S.V. Hoffmann:** Writing – review & editing, Supervision, Investigation, Funding acquisition, Data curation, Conceptualization. **M.H.F. Bettega:** Writing – review & editing, Writing – original draft, Software, Funding acquisition. **P. Limão-Vieira:** Writing – review & editing, Writing – original draft, Supervision, Funding acquisition, Conceptualization.

Declaration of competing interest

The authors declare that they have no known competing financial interests or personal relationships that could have appeared to influence the work reported in this paper.

Acknowledgments

LVSD, EB and MHFB acknowledge the support from the Brazilian agencies Coordenação de Aperfeiçoamento de Pessoal de Nível Superior (CAPES) and Conselho Nacional de Desenvolvimento Científico e Tecnológico (CNPq). LVSD, EB and MHFB also acknowledge Prof. Carlos A. M. de Carvalho for computational support at LFTC-DFis-UFPR. The authors wish to acknowledge the beam time at the ISA synchrotron, Aarhus University, Denmark. The research leading to this result has been supported by the project CALIPSOplus under the Grant Agreement 730872 from the EU Framework Programme for Research and Innovation HORIZON 2020. PL*V* acknowledges the Portuguese National Funding Agency (FCT) through research grant CEFITEC (UID/00068) and his visiting professor position at Federal University of Paraná, Curitiba, Brazil.

Appendix A. Supplementary material

Supplementary data to this article can be found online at https://doi.org/10.1016/j.cplett.2025.142075.

Data availability

Data will be made available on request.

References

[1] F.F. Silva, D. Almeida, G. Martins, A.R. Milosavljević, B.P. Marinković, S. V. Hoffmann, N.J. Mason, Y. Nunes, G. Garcia, P. Limão-Vieira, The electronic states of pyrimidine studied by VUV photoabsorption and electron energy-loss spectroscopy, Phys. Chem. Chem. Phys. 12 (2010) 6717–6731, https://doi.org/10.1039/b927412j.

[2] M. Sala, M. Saab, B. Lasorne, F. Gatti, S. Guérin, Laser control of the radiationless decay in pyrazine using the dynamic stark effect, J. Chem. Phys. 140 (2014) 194309, https://doi.org/10.1063/1.4875736.

[3] M. Sala, S. Guérin, F. Gatti, Quantum dynamics of the photostability of pyrazine, Phys. Chem. Chem. Phys. 17 (2015) 29518–29530, https://doi.org/10.1039/c5cp04605j.

[4] J.D. Simmons, K.K. Innes, Infrared and Raman spectra of pyrazine-h4 and-d4, J. Mol. Spectrosc. 14 (1964) 190–197, https://doi.org/10.1016/0022-2852(64)90113-4.

[5] K.B. Hewett, M. Shen, C.L. Brummel, L.A. Philips, High resolution infrared spectroscopy of pyrazine and naphthalene in a molecular beam, J. Chem. Phys. 100 (1994) 4077–4086, https://doi.org/10.1063/1.466345.

[6] M. Ito, R. Shimada, T. Kuraishi, W. Mizushima, Ultraviolet absorption of pyrazine vapor due to n-π transition, J. Chem. Phys. 26 (1957) 1508–1515, https://doi.org/10.1063/1.1743570.

[7] J.E. Parkin, K.K. Innes, The vacuum ultraviolet spectra of pyrazine, pyrimidine, and Pyridazine vapors part I. Spectra between 1550 Å and 2000 Å, J. Mol. Spectrosc. 16 (1965) 407–434, https://doi.org/10.1016/0022-2852(65)90001-9.

[8] A. Bolovinos, P. Tsekeris, J. Philis, E. Pantos, G. Andritsopoulos, Absolute vacuum ultraviolet absorption spectra of some gaseous azabenzenes, J. Mol. Spectrosc. 103 (1984) 240–256, https://doi.org/10.1016/0022-2852(84)90051-1.

[9] M. Stener, P. Decleva, D.M.P. Holland, D.A. Shaw, A study of the valence shell electronic states of pyrimidine and pyrazine by photoabsorption spectroscopy and time-dependent density functional theory calculations, J. Phys. B Atomic Mol. Phys. 44 (2011) 075203, https://doi.org/10.1088/0953-4075/44/7/075203.

[10] I. Suzuka, Y. Udagawa, M. Ito, Raman spectra of pyrazine resonant to the S2(π,π*) state and the geometry in excited state, Chem. Phys. Lett. 64 (1979) 333–336, https://doi.org/10.1016/0009-2614(79)80525-4.

[11] I.C. Walker, M.H. Palmer, The electronic states of the azines. IV. Pyrazine, studied by VUV absorption, near-threshold electron energy-loss spectroscopy and ab initio multi-reference configuration interaction calculations, Chem. Phys. 153 (1991) 169–187, https://doi.org/10.1016/0301-0104(91)90017-N.

[12] I. Yamazaki, T. Murao, T. Yamanaka, K. Yoshihara, Intramolecular electronic relaxation and photoisomerization processes in the isolated azabenzene molecules pyridine, pyrazine and pyrimidine, Faraday Discuss. Chem. Soc. 75 (1983) 395–405, https://doi.org/10.1039/DC9837500395.

[13] B. Samir, C. Kalalian, E. Roth, R. Salghi, A. Chakir, Gas-phase UV absorption spectra of pyrazine, pyrimidine and pyridazine, Chem. Phys. Lett. 751 (2020) 137469, https://doi.org/10.1016/j.cplett.2020.137469.

[14] P. Esherick, P. Zinsli, M.A. El-Sayed, The low energy two-photon Spectrum of pyrazine using the phosphorescence photoexcitation method, Chem. Phys. 10 (1975) 415–432, https://doi.org/10.1016/0301-0104(75)87053-4.

[15] A. Amirav, Rotational effects on pyrazine S1 (1B3u) dynamics. III. Vibrational energy effect and the transition from small molecule to statistical limit, Chem. Phys. 126 (1988) 365–375, https://doi.org/10.1016/0301-0104(88)85044-4.

[16] H. Baba, N. Ohta, O. Sekiguchi, M. Fujita, K. Uchida, Effects of molecular rotation on electronic relaxation processes in pyrazine and pyrimidine with particular regard to pressure dependence, J. Phys. Chem. 87 (1983) 943–952, https://doi.org/10.1021/j100229a009.

[17] S.N. Thakur, K.K. Innes, Reassignment of the “forbidden” character in the A1B3u-XlAg transitions of pyrazine-d0,15N and d41, J. Mol. Spectrosc. 52 (1974) 130–145, https://doi.org/10.1016/0022-2852(74)90009-5.

[18] J.E. Del Bene, J.D. Watts, R.J. Bartlett, Coupled-cluster calculations of the excitation energies of benzene and the azabenzenes, J. Chem. Phys. 106 (1997) 6051–6060, https://doi.org/10.1063/1.473245.

[19] R. He, C. Zhu, C.H. Chin, S.H. Lin, Ab initio studies of excited electronic state S2 of pyrazine and Franck-Condon simulation of its absorption spectrum, Chem. Phys. Lett. 476 (2009) 19–24, https://doi.org/10.1016/j.cplett.2009.05.043.

[20] C.K. Lin, Y. Niu, C. Zhu, Z. Shuai, S.H. Lin, The role of the nπ* 1Au state in the photoabsorption and relaxation of pyrazine, Chem. Asian J. 6 (2011) 2977–2985, https://doi.org/10.1002/asia.201100472.

[21] T. Shiozaki, C. Woywod, H.J. Werner, Pyrazine excited states revisited using the extended multi-state complete active space second-order perturbation method, Phys. Chem. Chem. Phys. 15 (2013) 262–269, https://doi.org/10.1039/c2cp43381h.

[22] C. Woywod, W. Domcke, A.L. Sobolewski, H.J. Werner, Characterization of the S1-S2 conical intersection in pyrazine using ab initio multiconfiguration self-consistent-field and multireference configuration-interaction methods, J. Chem. Phys. 100 (1994) 1400–1413, https://doi.org/10.1063/1.466618.

[23] M. Sala, B. Lasorne, F. Gatti, S. Guérin, The role of the low-lying dark nπ* states in the photophysics of pyrazine: a quantum dynamics study, Phys. Chem. Chem. Phys. 16 (2014) 15957–15967, https://doi.org/10.1039/c4cp02165g.

[24] L. Åsbrink, E. Lindholm, O. Edqvist, Jahn-teller effect in the vibrational structure of the photoelectron soectrum of benzene, Chem. Phys. Lett. 5 (1970) 609–612, https://doi.org/10.1016/0009-2614(70)85060-6.

[25] C. Fridh, L. Åsbrink, B.Ö. Jonsson, E. Lindholm, X.V. Photoelectron, UV, mass and electron impact spectra of pyrazine, Int. J. Mass Spectrom. Ion Process. 8 (1972) 101–118, https://doi.org/10.1016/0020-7381(72)80002-0.

[26] D.M.P. Holland, A.W. Potts, L. Karlsson, M. Stener, P. Decleva, A study of the valence shell photoionisation dynamics of pyrimidine and pyrazine, Chem. Phys. 390 (2011) 25–35, https://doi.org/10.1016/j.chemphys.2011.09.025.

[27] T. Horio, Y.I. Suzuki, T. Suzuki, Ultrafast photodynamics of pyrazine in the vacuum ultraviolet region studied by time-resolved photoelectron imaging using 7.8-eV pulses, J. Chem. Phys. 145 (2016) 044307, https://doi.org/10.1063/1.4955298.

[28] T. Horio, R. Spesyvtsev, K. Nagashima, R.A. Ingle, Y.I. Suzuki, T. Suzuki, Full observation of ultrafast cascaded radiationless transitions from S2(ππ-) state of pyrazine using vacuum ultraviolet photoelectron imaging, J. Chem. Phys. 145 (2016) 044306, https://doi.org/10.1063/1.4955296.

[29] S. Eden, P. Limão-Vieira, S.V. Hoffmann, N.J. Mason, VUV photoabsorption in CF3X (X = cl, Br, I) fluoro-alkanes, Chem. Phys. 323 (2006) 313–333.

[30] M.H. Palmer, T. Ridley, S.V. Hoffmann, N.C. Jones, M. Coreno, M. De Simone, C. Grazioli, M. Biczysko, A. Baiardi, P. Limão-Vieira, Interpretation of the vacuum ultraviolet photoabsorption spectrum of iodobenzene by ab initio computations, J. Chem. Phys. 142 (2015) 134302.

[31] D. Duflot, S.V. Hoffmann, N.C. Jones, P. Limão-Vieira, Synchrotron radiation UV-VUV photoabsorption of gas phase molecules, in: A.S. Pereira, P. Tavares, P. Limão-Vieira (Eds.), Radiation in Bioanalysis: Spectroscopic Techniques and Theoretical Methods, Springer, 2019, pp. 43–81.

[32] R. Bauernschmitt, R. Ahlrichs, Treatment of electronic excitations within the adiabatic approximation of time dependent density functional theory, Chem. Phys. Lett. 256 (1996) 454–464.

[33] M.E. Casida, Time-dependent density-functional theory for molecules and molecular solids, J. Mol. Struct.-Theochem. 914 (2009) 3–18.

[34] B. Miehlich, A. Savin, H. Stoll, H. Preuss, Results obtained with the correlation energy Density Functionals of Becke and Lee, Yang and Parr, Chem. Phys. Lett. 157 (1989) 200–206, https://doi.org/10.1016/0009-2614(89)87234-3.

[35] A.D. Becke, Density-functional exchange-energy approximation with correct asymptotic behavior, Phys. Rev. A 38 (1988) 3098–3100, https://doi.org/10.1103/PhysRevA.38.3098.

[36] A.D. Becke, Density-functional thermochemistry. V. Systematic optimization of exchange-correlation functionals, J. Chem. Phys. 107 (1997) 8554–8560, https://doi.org/10.1063/1.475007.

[37] A.D. Becke, Density-functional thermochemistry. IV. A new dynamical correlation functional and implications for exact-exchange mixing, J. Chem. Phys. 104 (1996) 1040–1046, https://doi.org/10.1063/1.470829.

[38] A.D. Becke, Density-functional thermochemistry. III. The role of exact exchange, J. Chem. Phys. 98 (1993) 5648–5652, https://doi.org/10.1063/1.464913.

[39] A.D. Becke, Exploring the limits of gradient corrections in Density functional theory, J. Comput. Chem. 20 (1999) 63–69, 10.1002/(SICI)1096-987X(19990115)20:1<63::AID-JCC8>3.0.CO;2-A.

[40] C. Lee, W. Yang, R.G. Parr, Development of the Colle-Salvetti correlation-energy formula into a functional of the electron density, Phys. Rev. B 37 (1988) 785–789, https://doi.org/10.1103/PhysRevB.37.785.

[41] R.A. Kendall, T.H. Dunning, R.J. Harrison, Electron affinities of the first-row atoms revisited. Systematic basis sets and wave functions, J. Chem. Phys. 96 (1992) 6796–6806, https://doi.org/10.1063/1.462569.

[42] G.M.J. Barca, C. Bertoni, L. Carrington, D. Datta, N. De Silva, J.E. Deustua, D. G. Fedorov, J.R. Gour, A.O. Gunina, E. Guidez, T. Harville, S. Irle, J. Ivanic, K. Kowalski, S.S. Leang, H. Li, W. Li, J.J. Lutz, I. Magoulas, J. Mato, V. Mironov, H. Nakata, B.Q. Pham, P. Piecuch, D. Poole, S.R. Pruitt, A.P. Rendell, L.B. Roskop, K. Ruedenberg, T. Sattasathuchana, M.W. Schmidt, J. Shen, L. Slipchenko, M. Sosonkina, V. Sundriyal, A. Tiwari, J.L. Galvez Vallejo, B. Westheimer, M. Włoch, P. Xu, F. Zahariev, M.S. Gordon, Recent developments in the general atomic and molecular electronic structure system, J. Chem. Phys. 152 (2020) 154102.

[43] C. Adamo, V. Barone, Toward reliable density functional methods without adjustable parameters: the PBE0 model, J. Chem. Phys. 110 (1999) 6158–6170, https://doi.org/10.1063/1.478522.

[44] T. Yanai, D.P. Tew, N.C. Handy, A new hybrid exchange-correlation functional using the Coulomb-attenuating method (CAM-B3LYP), Chem. Phys. Lett. 393 (2004) 51–57, https://doi.org/10.1016/j.cplett.2004.06.011.

[45] D.O. Kashinski, G.M. Chase, R.G. Nelson, O.E. Di Nallo, A.N. Scales, D. L. Vanderley, E.F.C. Byrd, Harmonic vibrational frequencies: approximate global scaling factors for TPSS, M06, and M11 functional families using several common basis sets, J. Phys. Chem. A 121 (2017) 2265–2273, https://doi.org/10.1021/acs.jpca.6b12147.

[46] K.K. Innes, I.G. Ross, W.R. Moomaw, Electronic states of azabenzenes and azanaphthalenes: a revised and extended critical review, J. Mol. Spectrosc. 132 (1988) 492–544, https://doi.org/10.1016/0022-2852(88)90343-8.

[47] B.M. Bode, M.S. Gordon, MacMolPlt: a graphical user interface for GAMESS, J. Mol. Graphics Mod. 16 (1998) 133–138, https://doi.org/10.1016/S1093-3263(99)00002-9.